Max-Planck-Institut
für Mathematik
in den Naturwissenschaften
Leipzig

Characterizing Complex Networks with Forman-Ricci Curvature and Associated Geometric Flows

(revised version: October 2016)

by

Melanie Weber, Emil Saucan, and Jürgen Jost

Characterizing Complex Networks with Forman-Ricci curvature and associated geometric flows

Melanie Weber[1,2], Emil Saucan[1,3] and Jürgen Jost [1,4]

[1] Max-Planck-Institute for Mathematics in the Sciences; Inselstrasse 22, 04103 Leipzig, Germany
[2] Mathematical Institute, University of Leipzig; Augustusplatz 10, 04109 Leipzig, Germany
[3] Technion - Israel Institute of Technology; Haifa 32000, Israel
[4] Santa Fe Institute; 1399 Hyde Park Road Santa Fe, New Mexico 87501 USA
(Contact: melweber@t-online.de, semil@ee.technion.ac.il, jost@mis.mpg.de)

October 18, 2016

Abstract

We introduce Forman-Ricci curvature and its corresponding flow as characteristics for complex networks attempting to extend the common approach of node-based network analysis by edge-based characteristics. Following a theoretical introduction and mathematical motivation, we apply the proposed network-analytic methods to static and dynamic complex networks and compare the results with established node-based characteristics. Our work suggests a number of applications for data mining, including denoising and clustering of experimental data, as well as extrapolation of network evolution. Complex networks, Forman-Ricci-curvature, Ricci-flow, Laplacian flow, data mining
2000 Math Subject Classification: 05C82, 05C75, 05C21, 05C10

Contact: mw25@math.princeton.edu, semil@ee.technion.ac.il, jost@mis.mpg.de

1 Introduction

Network graphs have been perceived as practical models for complex systems for decades. With the rapid rise of data science since the late 1990s, they have become a widely used form of data representation that is easily storable and can be effectively analyzed with data mining methods.

Complex networks represent a wide variety of data sets and systems, ranging from social interactions in large online social networks like Facebook and Twitter to neuronal activities in cortical graphs and genetic interactions in the human genome. Outside the social and natural sciences, networks are used as models for the spread of information in the world wide web and the shared use of energy ressources – to name just a few examples.

Since the early days of network sciences, there have been numerous attempts to characterize complex real-world networks with standard models that capture essential topological properties. Most notably are the models of P. Erdős and A. Rényi [Erdős and Rényi, 1959, Erdős and Rényi, 1960], D. Watts and S. Strogatz [Watts and Strogatz, 1998] and R. Albert and A. Barabási [Barabási and Albert, 1999]. Their efforts were addressed with both praise

(e.g. [Amaral et al., 2000, Jeong et al., 2000]) and concerns (e.g. [Arita, 2004, Lee et al., 2015]) in the literature in terms of their capabilities as well as deficiencies in describing real world systems.

Common among most network models is the focus on node degree distributions, clustering coefficiants and the average path length as the defining topological and geometrical properties [Strogatz, 2006, Newman, 2003]. More recently [Gu et al., 2016, Banerjee and Jost, 2008], the spectrum of the normalized graph Laplacian has been introduced as a useful classification scheme. In this work, we suggest additional edge-based characteristics based on combinatorial approaches, namely the Forman-Ricci curvature and the Bochner Laplacian, as well as their corresponding flows.

Until quite recently, Ricci curvature has been just one of the various curvature notions in Riemannian Geometry, best known for its role in Einstein's field equations. However, this has changed drastically due to the spectacular mathematical applications in G. Perelman's far reaching work on the Ricci flow and the Geometrization Conjecture [Perelman, 2002, Perelman, 2003].

While started far earlier [Stone, 1976], the search for the discretization of this notion has gained fast momentum, spurred by Perelman's groundbreaking results. One notable approach is that of Chow and Luo [Chow and Luo, 2003], based on circle packings. It has been successfully applied in Graphics, Medical Imaging and Communication Networks (see e.g. [Yin et al., 2008]) giving rise to many practical applications. A radically different approach was adopted by Ollivier [Ollivier, 2009, Ollivier, 2010], that proved to be excellently suited for modeling Complex Networks, both from the theoretical [Bauer et al., 2012, Jost and Liu, 2014, Loisel and Romon, 2014], as well as applied [Sandhu et al., 2015a, Sandhu et al., 2015b, Ni et al., 2015, Li et al., 2014] viewpoints.

Recently, another discretization of Ricci curvature for complex networks based on Forman's theoretical work [Forman, 2003] has been introduced [Sreejith et al., 2016a, Sreejith et al., 2016b, Weber et al., 2016]. While based on different ideas than those residing at the base of Ollivier's discretization, Forman's version is far simpler to implement - an advantage that was emphasized and exploited in the papers mentioned above. Furthermore, there are strong theoretical indications that the two approaches are closely correlated, suggesting to substitute Ollivier's curvature with Forman's for efficient computation in practical applications.

The formalism discussed in the present article naturally applies to both static and dynamic networks. We discuss the duality of curvature and flow in a more general, theoretic setting and its exploitation in Network Analysis. Both concepts are used to investigate model and real-world networks, including web graphs (Google), social networks (Facebook) and biological networks (gene networks, BioGrid), in terms of the Ricci-formalism. The results are discussed in comparison to node-degree based network analysis and standard models as classifiers of complex networks representing real-world systems. In the second part of the article, we focus on characterizing dynamic networks with the help of the Ricci flow in an attempt to detect and describe the topological properties of the underlying dynamic effects. We evaluate our results in comparison to the Laplacian flow, a node-based method related to both the Forman curvature and the Bochner Laplacian.

We conclude with possible applications of the discussed methods in data mining with an emphasis on the analysis of dynamic effects in complex systems.

2 Forman-Ricci curvature and the Bochner Laplacian

In this section we will give a mathematical motivation and rigorous introduction of the Ricci-formalism for networks. We will discuss essential properties of Forman's Ricci curvature and the resulting important consequences for complex networks before moving on to possible practical applications in Network Analysis in the next sections.

2.1 Ricci curvature

In the classical, geometric sense, Ricci curvature measures the deviation of a manifold from being locally Euclidean in various tangential directions. More precisely, it quantifies both divergence (of geodesics) and (volume) growth in the second term of the $(n-1)$-dimensional volume $\Omega(\varepsilon)$ through controlling the growth of the measured angles, as quantified by the following classical formula:

$$\Omega(\varepsilon) = \text{Vol}\big(\varpi(\alpha)\big) = d\alpha\,\varepsilon^{n-1}\left(1 - \frac{\text{Ric}(\mathbf{v})}{3}\varepsilon^2 + o(\varepsilon^2)\right). \tag{1}$$

where $d\alpha$ denotes the n-dimensional solid angle in the direction of the vector $\mathbf{v} \in T_p(M^n)$ and $\varpi(\alpha)$ represents the $(n-1)$-volume generated by geodesics of length ε in $d\alpha$. Forman's discretization of the Ricci curvature specifically captures the volume growth and transfers the formalism to networks.
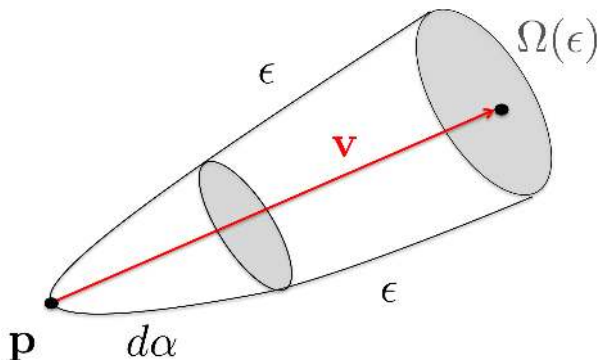

Figure 1: Ricci curvature as deviation of a manifold from being locally Euclidean in various tangential directions (after Berger [Berger, 2012]). Here $d\alpha$ denotes the solid angle in the direction of the vector $\mathbf{v}$, and Ω the volume generated by the geodesics of length ϵ in $d\alpha$.

Technically, Ricci curvature represents an average of *sectional curvatures*. As an analogy to the classical *mean curvature* of surfaces, this *averaging property* is further emphasized by the fact that Ricci curvature acts as the Laplacian of the metric g [Berger, 2012]. Notably, in dimension $n = 2$, i.e. in the case most relevant for classical Image Processing and related fields, Ricci curvature reduces to sectional (and scalar) curvature in the form of the classical case [Berger, 2012].

2.2 The Bochner Laplacian

Before proceeding to the more technical aspects, we note that Forman's definition has a quite general discrete setting. It is based on an abstraction of a classical formula known from Dif-

ferential Geometry and Geometric Analysis as the so called *Bochner-Weitzenböck formula* (see, e.g. [Jost, 2011]), for *weighted CW cell complexes*, an abstraction of both polygonal meshes and weighted graphs. This formula relates curvature to the classical (Riemannian) Laplace operator. In consequence, and as a byproduct of its very definition, Forman's Ricci curvature comes coupled with a fitting Laplacian (or, in fact, two Laplacians, as we shall see below). The parallelism of the Forman-curvature and the Bochner Laplacian, also reflected in the corresponding flows, has important implications on the transfer of theoretical results and possible applications onto various fields of Network Analysis.

In its best known form, for functions, the Bochner-Weitzenböck formula is written as:

$$-\frac{1}{2}\Delta\left(||df||^2\right) = ||\mathrm{Hess}f||^2 - <df, \Delta df> + \mathrm{Ric}(df, df).\tag{2}$$

Here $\mathrm{Hess}f$ denotes the Hessian of f: $\mathrm{Hess}f = \nabla df = \nabla^2 f$ and $<\cdot, \cdot>$ as usual, the inner product. A proof can be found, e.g., in [Jost, 2011][1]. However, there is no natural or general applicable interpretation of this form of the Bochner formula. Therefore, to generalize the notion of Ricci curvature to allow for a description of weighted cell complexes, one starts from the following form of the *Bochner-Weitzenböck* formula (see, e.g. [Berger, 2012, Jost, 2011]) for the *Riemann-Laplace operator* $\Box_p$ on p-forms on (compact) Riemannian manifolds:

$$\Box_p = dd^* + d^*d = \nabla_p^*\nabla_p + \mathrm{Curv}(R),\tag{3}$$

where $\nabla_p^*\nabla_p$ is the *Bochner* (or *rough*) *Laplacian* and $\mathrm{Curv}(R)$ an expression of the *curvature tensor* with linear coefficients where ∇_p denotes the *covariant derivative* operator. For cell-complexes, one of course cannot expect the existence of such differentiable operators. However, a *formal* differential exists: In our combinatorial context (the operator) "d" being replaced by "∂" – the boundary operator of the cellular chain complex (see [Kaczynski et al., 2004]), we have

$$0 \to C_n(M, \mathbb{R}) \xrightarrow{\partial} C_{n-1}(M, \mathbb{R}) \xrightarrow{\partial} \cdots \xrightarrow{\partial} C_0(M, \mathbb{R}) \to 0,$$

where cells are analogues of forms in the classical (i.e. Riemannian) setting. The following definition of the Bochner Laplacian becomes now natural:

$$\Box_p = \partial\partial^* + \partial^*\partial : C_p(M, \mathbb{R}) \to C_p(M, \mathbb{R}),\tag{4}$$

where $\partial^* : C_p(M, \mathbb{R}) \to C_{p+1}(M, \mathbb{R})$ is the *adjoint* (or *coboundary*) operator of ∂, defined by: $<\partial_{p+1}c_{p+1}, c_p> = <c_{p+1}, \partial_p^* c_p>_{p+1}$, where $<\cdot, \cdot> = <\cdot, \cdot>_p$ is a (positive definite) inner product on $C_p(M, \mathbb{R})$, i.e. satisfying: (i) $<\alpha, \beta> = 0, \forall\alpha \neq \beta$ and (ii) $<\alpha, \alpha> = w_\alpha > 0$ – the weight of cell α.

Forman [Forman, 2003] (see also the much earlier [Eckmann, 1944]) shows that an analogue of the Bochner-Weitzenböck formula holds in this setting, i.e. that there exists a canonical decomposition of the form:

$$\Box_p = B_p + F_p,\tag{5}$$

---

[1] Besides proofing the above statement, [Jost, 2011] emphasizes the role of Ricci curvature in the formula of the Jacobian determinant of the exponential map, thus underlining the role of Ricci curvature as a measure of growth – see also the observation above regarding this very aspect of Forman's discretization.

where B_p is a *non-negative operator* and F_p is a diagonal matrix. $\square_p$, B_p and F_p are called, in analogy with the classical Bochner-Weitzenböck formula, the *combinatorial Riemann-Laplace operator*, the *combinatorial Bochner* (or *rough*) *Laplacian*, and the *combinatorial curvature function*, respectively.

If $\alpha = \alpha^p$ is a p-dimensional cell (or p-cell, for short), then we can define the *curvature function* $F_p : C_p \to C_p$

$$\mathcal{F}_p = < F_p(\alpha), \alpha >, \tag{6}$$

as a linear function on p-chains. For dimension $p = 1$ we obtain, by analogy with the classical case, the following definition of discrete (weighted) *Forman-Ricci curvature* on $\alpha = \alpha^1$, i.e. 1-cells (edges):

$$\mathrm{Ric}_\mathrm{F}(\alpha) = \mathcal{F}_1(\alpha). \tag{7}$$

The formalism does not restrict the choice of the weight function, i.e. it allows for general weights making the Forman-Ricci curvature extremely versatile. A handy choice are the so called *standard weights* [Forman, 2003], that generalize the intuitive geometric notions of length, area and volume:

$$w(\alpha^p) = w_1 \cdot w_2^p. \tag{8}$$

Note that the *combinatorial weights* $w_\alpha \equiv 1$ represent a set of standard weights, with $w_1 = w_2 = 1$.

Using the properties of standard weights and their relationship with generic weights, we obtain the following formula for polyhedral (and in fact much more general) complexes, endowed with any set of (positive) weights:

$$\mathcal{F}(\alpha^p) = w(\alpha^p) \Big[\Big(\sum_{\beta^{p+1} > \alpha^p} \frac{w(\alpha^p)}{w(\beta^{p+1})} + \sum_{\gamma^{p-1} < \alpha^p} \frac{w(\gamma^{p-1})}{w(\alpha^p)} \Big) \tag{9}$$

$$- \sum_{\alpha_1^p \| \alpha^p, \alpha_1^p \neq \alpha^p} \Big| \sum_{\substack{\beta^{p+1} > \alpha_1^p \\ \beta^{p+1} > \alpha^p}} \frac{\sqrt{w(\alpha^p)w(\alpha_1^p)}}{w(\beta^{p+1})} - \sum_{\substack{\gamma^{p-1} < \alpha_1^p \\ \gamma^{p-1} < \alpha^p}} \frac{w(\gamma^{p-1})}{\sqrt{w(\alpha^p)w(\alpha_1^p)}} \Big| \Big];$$

with $\alpha < \beta$ meaning that α is a face of β, and $\alpha_1 \| \alpha_2$ signifying the simplices α_1 and α_2 to be *parallel*.
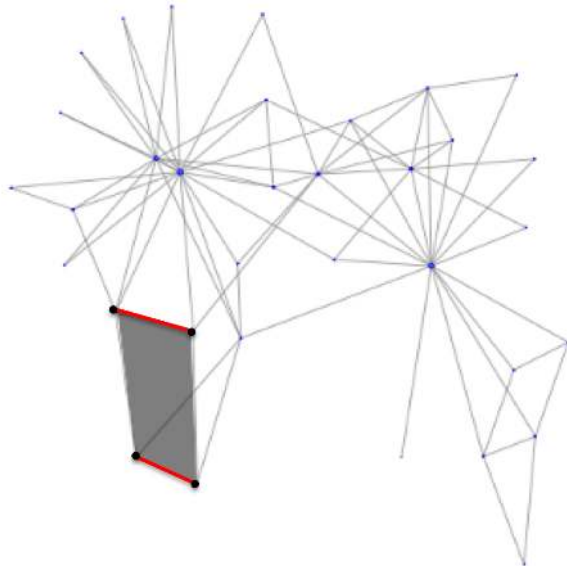
Figure 2: Social network [Zachary, 1977] with highlighted cells. Parallel cells (edges: red), with distinct children (nodes: black) and a common parent (face: gray).

Parallel cells are precisely those that either have a common "*parent*" (adjacent higher dimensional face) or a common "*child*" (adjacent lower dimensional face), but not those that have both a common parent and common child (see Fig. (2)). Together with the formula above, the combinatorial Riemann-Laplace operator (see [Forman, 2003]) is also obtained, when we consider the Laplacian written in not necessarily symmetric form (although, with a suitable choice of an inner product, the Laplacian is a symmetric operator, see [Horak and Jost, 2013]), as:

$$\Box_p(\alpha_1^p, \alpha_2^p) = \sum_{\substack{\beta^{p+1} > \alpha_1^p \\ \beta^{p+1} > \alpha_2^p}} \epsilon_{\alpha_1,\alpha_2,\beta} \frac{\sqrt{w(\alpha_1^p)w(\alpha_2^p)}}{w(\beta^{p+1})} + \sum_{\substack{\gamma^{p-1} < \alpha_1^p \\ \gamma^{p-1} < \alpha_2^p}} \epsilon_{\alpha_1,\alpha_2,\gamma} \frac{w(\gamma^{p-1})}{\sqrt{w(\alpha_1^p)w(\alpha_2^p)}} ; \quad (10)$$

where $\epsilon_{\alpha_1,\alpha_2,\beta}, \epsilon_{\alpha_1,\alpha_2,\gamma} \in \{-1, +1\}$ are the relative orientations of the cells.

Remark. One might object that the formulas above hold only for the case of standard weights, whereas weights associated to intrinsic information in the real data need not necessarily satisfy such dimensionality scaling – like the one displayed by area and volume with respect to the length, as encapsulated by condition (8). In particular, while this scaling holds for polygonal and polyhedral meshes, it does not necessarily hold for networks. However, an important result of Forman ([Forman, 2003], Theorem 2.5) consist precisely in showing that, for an open, dense set of weights, the essential property required for the formulas in question to hold is satisfied. Therefore, while the given weights might not satisfy the required property themselves, there exist weights arbitrarily close to them that do. Hence they can replace, formally, the given ones, without any perceivable computational error.

2.3 The case of networks

In 1-dimensional regular CW-complexes, such as networks or locally finite graphs, there are no faces of dimension higher than one. It follows for these cases including the complex networks considered here, that edges have no "parents", but only "children" (nodes). This observation

6

greatly simplifies (9), since it causes half of the terms to vanish. The case in which we do have these higher (and lower) order structures will be covered in a forthcoming article by the authors.

By further taking $p = 1$, we obtain the Forman-Ricci curvature for networks:

$$\text{Ric}_F(e) = \omega(e) \left(\frac{\omega(v_1)}{\omega(e)} + \frac{\omega(v_2)}{\omega(e)} - \sum_{\substack{e_{v_1} \sim e \\ e_{v_2} \sim e}} \left[\frac{\omega(v_1)}{\sqrt{\omega(e)\omega(e_{v_1})}} + \frac{\omega(v_2)}{\sqrt{\omega(e)\omega(e_{v_2})}} \right] \right). \tag{11}$$

Analogously to (2.8), the Bochner Laplacian simplifies, for $p = 1$, to

$$\Box_1(e_1, e_2) = \sum_{\substack{e_1 \sim v \\ e_2 \sim v}} \frac{\omega(v)}{\sqrt{\omega(e_1)\omega(e_2)}}, \tag{12}$$

due to vanishing terms related to the non-occurrence of higher order faces. In section 4, we will use (11) and (12) to characterize the flow on networks.

As underlined above, the main advantage of Forman-Ricci curvature as a network characteristic resides in the fact that it is an edge based notion. However, it can be preferable to use a node based version. In that case, the Forman-Ricci curvature of a node can be defined as the sum of the curvatures of all edges incident to that node:

$$\mathbf{F}(v) = \sum_{e_v \sim v} \mathbf{F}(e_v). \tag{13}$$

Directed (oriented) networks are essential for modeling a variety of phenomena, such as those included in the experimental part of the present paper (see Section 3). However, in Forman's original work, the weights (as generalizations of length, area, etc.) were taken to be positive. Hence, the Forman-Ricci curvature is not directly applicable for non-orientable surfaces (or, more generally, manifolds/ cell complexes). However, one can adapt its notion from undirected to directed graphs by rearranging the terms in the definition of the Forman curvature for an edge e (Eq. 11), and write the contributions of the two adjacent nodes v_1 and v_2 separately (see also [Sreejith et al., 2016b]) as

$$\mathbf{F}(e) = w_e \left(\frac{w_{v_1}}{w_e} - \sum_{e_{v_1} \sim e} \frac{w_{v_1}}{\sqrt{w_e w_{e_{v_1}}}} \right) + w_e \left(\frac{w_{v_2}}{w_e} - \sum_{e_{v_2} \sim e} \frac{w_{v_2}}{\sqrt{w_e w_{e_{v_2}}}} \right). \tag{14}$$

Note, that this naturally defines the curvature of a directed edge by only using the term involving its initial node, or alternatively its terminal node.

This definition can be, in turn, easily adapted to nodes: Given a node v, let us denote the set of *incoming* and *outgoing* edges of v by $E_{I,v}$ and $E_{O,v}$, respectively. Then, one can define the *In Forman curvature* $\text{Ric}_{F,I}(v)$ and the *Out Forman curvature* $\text{Ric}_{F,O}(v)$ as follows:

$$\text{Ric}_{F,I}(v) = \sum_{e \in E_{I,v}} \text{Ric}_{F,I}(e); \tag{15}$$

$$\text{Ric}_{F,O}(v) = \sum_{e \in E_{O,v}} \text{Ric}_{F,O}(e); \tag{16}$$

where the summations are taken over only the incoming and outgoing edges, respectively. Moreover, one can obtain the total amount of flow through a node v as follows:

$$\text{Ric}_{\text{F,I/O}}(v) = \text{Ric}_{\text{F,I}}(v) - \text{Ric}_{\text{F,O}}(v). \tag{17}$$

Note that we extend formula (2.8) and define the Ricci curvature of a directed edge, by using just one of its two nodes, i.e. either its "head" or its "tail". Here we measure the incoming edges at the head and the outgoing ones at the tail where directions are defined from head to tail. While there are other possible choices, we preferred this convention, as it is the most natural for modeling a variety the networks, in particular those analyzed in the present article.

3 Application on Complex Networks

In the previous section, the Forman-Ricci curvature was rigorously introduced as a network property. Now we want to investigate its applicability as a characteristic for real-world complex networks.

As already noted above, common network characteristics are usually node-based features, i.e. greatly dependent on node-degrees. While there are a great number of proposed approaches, typically, the node degree distribution, the average path length between any two nodes and the clustering coefficient [Newman, 2003] are used as "gold standards" for evaluating and classifying networks (a notable exception to this common approach can be found in [Bai et al., 2016]). All of these properties are highly dependent on node degrees, over-emphasizing the structural importance of nodes over edges.

This exaggerated centrality of node degree-based features holds also for the three most established model networks (respectively, Erdős-Rényi [Erdős and Rényi, 1959, Erdős and Rényi, 1960], Watts-Strogatz [Watts and Strogatz, 1998] and Albert-Barabási [Barabási and Albert, 1999]), that are widely used as exemplary models for real-world networks. Their common focus on node-based network properties has been both apprised [Amaral et al., 2000, Jeong et al., 2000] – for their simplicity – and criticized [Arita, 2004, Lee et al., 2015] – for significant qualitative deviations from real world networks.

In contrast, in this article, we examine the applicability of the edge-based Forman-Ricci curvature as a characteristic for complex networks. Many real-world networks are naturally weighted and other than in the case of standard weights imposed onto unweighted networks, we assume edge weights to be independent of node degrees. However, it has been shown that many weighted real-world networks, especially biological ones, have a node degree bias (see, e.g. [Ballouz et al., 2016] and the references therein). Even if curvature cannot be assumed independent of node degrees, it balances their dominance in network analysis by taking other important information - namely the edge weights - into account. We believe, that an extended network analysis that goes beyond the classic "gold standard" of network properties to include the curvature and possibly the spectrum of the graph Laplacian [Gu et al., 2016, Banerjee and Jost, 2008], gives a more complete picture and provides better insight into the topology of complex networks.

For the exploratory investigation of complex networks in this section, we follow current

developments and areas of major interest in the network sciences and related fields and choose the following exemplary data sets:

1. **Webgraphs**
   Following the increasing impact of the World Wide Web on today's world, the topology of the internet has attracted major interest in recent years. We investigate a Google web graph from [Palla et al., 2007, Kunegis, 2013], where nodes represent web pages and edges the respective hyperlinks between them.

2. **Social graphs**
   The rapid rise of social networks like Facebook, LinkedIn and Twitter have provided the social sciences with fundamentally new ways to study human interactions and social structures. Research now focuses on questions closely related to the topology of social graphs that represent the underlying complex systems. In this section, we study a Facebook friendship graph from [McAuley and Leskovec, 2012, Leskovec and Krevl, 2014], in which nodes denote users and edges represent the connections (friendships) between them.

3. **Biological networks**
   In recent years, data mining and network analysis have revolutionized a great number of disciplines in the biological sciences. For instance, networks built from co-expression data or protein-protein interactions in Genomics as well as brain networks in Neurosciences are widely used data representations that have given rise to fundamentally new methods and scientific approaches. Besides novel insights, these methods also demonstrate a need to understand the topology of networks for constructing null models and reliable means to account for noise biases that are an unavoidable feature of systems modeled from experimental data (see, e.g. [Ballouz et al., 2016] and the references therein). Here, we investigate a gene-interaction network built from BioGrid [Stark et al., 2006], where genes are represented by nodes and their associations and commonalities by the respective edges.

3.1 Forman-Ricci curvature as a network characteristic

Complex Networks

In this article, we consider network graphs

$$G = \{V, E\} \, ,$$

where $V(G)$ represents the set of nodes (or vertices) and $E(G)$ the edges connecting them according to known associations, interactions or commonalities. Those can be inferred from a given data set, empirical information or previous knowledge.

We impose a weighting scheme on the nodes

$$\omega : V(G) \mapsto [0, 1] \, , \tag{18}$$

that can reflect additional knowledge about the nodes (such as hierarchical positions in social networks, or the number of monthly visitors of a webpage) or - if no previous information on

the data points, other than their associations is given - we construct them combinatorial, based on node degrees:

$$\omega(v) = \frac{1}{\deg(v)} \sum_{u \sim v} \deg(u) \ . \tag{19}$$

To account for the strength of these associations, we define a normalized weighting scheme

$$\gamma : E(G) \mapsto [0, 1] \ . \tag{20}$$

The weights can be imposed directly from the given data (e.g. in correlation networks, as the correlation between two data points across a set of empirical data) or derived from the weights of the nodes they connect:

$$\gamma(e_{ij}) = \text{sign}(e_{ij}) \sqrt{\omega(v_i)^2 + \omega(v_j)^2} \ , \tag{21}$$

with

$$\text{sign}(e_{ij}) = \begin{cases} 1, & i \leq j \\ -1, & \text{else} \end{cases} \ . \tag{22}$$

The weighting scheme Eq.(21) is motivated by the geometric analogy of the distance between two points and can be extended to a more generalized weighting scheme for cellular complexes. Using edge and node weights, we can now determine the Forman curvature distribution from (11) (or, in the directed case, from (15) and (16)). For evaluation of the distribution, we use both histograms and curvature maps, the later ones containing through their spatial components additional information on directionality and community structure.

A curvature-based distance measure for graphs

Using the distribution of the Forman-Ricci curvature we want to introduce a tool for determining the distance between network graphs. We introduce a curvature-based pseudo-distance as a measure of the dissimilarity of pairs of graphs that gives rise to a curvature-based classification scheme.

Firstly, we estimate the density of the distribution through a (normalized) kernel density estimator

$$f_G : \text{Ric}_F(G) \to \mathbb{R} \ ; \tag{23}$$

$$f_G(e) = \frac{1}{|\hat{e}|} \sum_{\hat{e} \sim e} K \left(\text{Ric}_F(e) - \text{Ric}_F(\hat{e}) \right) \ , \tag{24}$$

with a kernel function K. Here, $\hat{e}$ are edges parallel to e. To characterize the distance between a pair of network graphs G_1 and G_2, we want to calculate the distance between the respective density estimates f_{G_1} and f_{G_1}. A distance measure for distributions is given by the *Wasserstein-*

distance [Gibbs and Su, 2002]

$$d_W^p = \inf \mathbb{E}\left(d\left(f_{G_1}, f_{G_2}\right)^{1/p}\right) \tag{25}$$

$$= \left(\int_{\mathbb{R}} |f_{G_1}(x) - f_{G_2}(x)|^p dx\right)^{1/p} . \tag{26}$$

Here, we will use a special form of the Wasserstein-1 metric. For this, we formulate the graph distance as an optimal transport problem and use the *earth mover's distance*, i.e. d_W^1, that can be computed by the *Hungarian algorithm* [Rubner et al., 2000]. We define clusters by splitting $\mathrm{supp} f_{G_{1,2}}$ into $k_{1,2}$ *bins*, i.e. curvature-intervals $\{x_{1,2}^i\}_{i=1,...,k}$ such that

$$\bigcup_{i=1}^{k} x_{1,2}^i = \mathrm{supp} f_{G_{1,2}} . \tag{27}$$

Each bin defines a cluster $P_{G_{1,2}} = \{P_{1,2}^1, ..., P_{1,2}^{k_1,k_2}\}$ where $P_{1,2}^i$ is characterized by a representative $p_{1,2}^i$ with weight $\omega(p_{1,2}^i)$, i.e.

$$p_{1,2}^i = \langle x_{1,2}^i \rangle ; \tag{28}$$

$$\omega(p_{1,2}^i) = f_{G_1,G_2}\left(\langle x_{1,2}^i \rangle\right) ; \tag{29}$$

$$P_{1,2}^i = \left(p_{1,2}^i, \omega(p_{1,2}^i)\right) . \tag{30}$$

The pairwise distances between the binned clusters of both graphs are the entries of the so-called *ground distance matrix*

$$D = \{d_{ij}\}_{\substack{i=1,...,k_1 \\ j=1,...,k_2}} = \mathrm{dist}\left(p_1^i, p_2^j\right) , \tag{31}$$

The distance between the graphs can also be viewed as the (finite) minimal number of modifications (i.e. adding or removing edges or nodes) to transform G_1 into G_2. In our setting, this corresponds to an optimal transport problem between the sets of clusters P_{G_1} and P_{G_2}. We introduce the *transportation flow*

$$F = \{f_{ij}\}_{\substack{i=1,...,k_1 \\ j=1,...,k_2}} , \tag{32}$$

for characterizing the transformation of P_{G_1} to P_{G_2}. To find the optimal transport F, we minimize the *transport cost*

$$W\left(P_{G_1}, P_{G_2}, F\right) = \sum_{i=1}^{k_1} \sum_{j=1}^{k_2} f_{ij} \cdot d_{ij} . \tag{33}$$

The optimization is implemented by, e.g. the Hungarian algorithm [Rubner et al., 2000]. With the resulting optimal F, we can calculate the distance between G_1 and G_2 by the *discrete earth mover's distance*

$$EMD\left(P_{G_1}, P_{G_2}\right) = d_W^1 = \frac{\sum_{i=1}^{k_1} \sum_{j=1}^{k_2} f_{ij} d_{ij}}{\sum_{i=1}^{k_1} \sum_{j=1}^{k_2} f_{ij}} . \tag{34}$$

3.2 Computational Data Analysis

Distribution and Similarity

We computed[2] the distribution of the Forman-Ricci curvature for the three real-world examples described above, as well as computationally generated examples for three model networks ($\sim 20,000$ nodes each, see *Supplemental Material* for details). The results are displayed as histograms and estimated density functions (Fig. 3) and as curvature maps (Fig.4), respectively. To quantify the dissimilarity, between the networks, we use the curvature-based distance measure introduced in the previous section. For computational purposes, the density estimates and separation into bins can be chosen in direct analogy to the histograms.
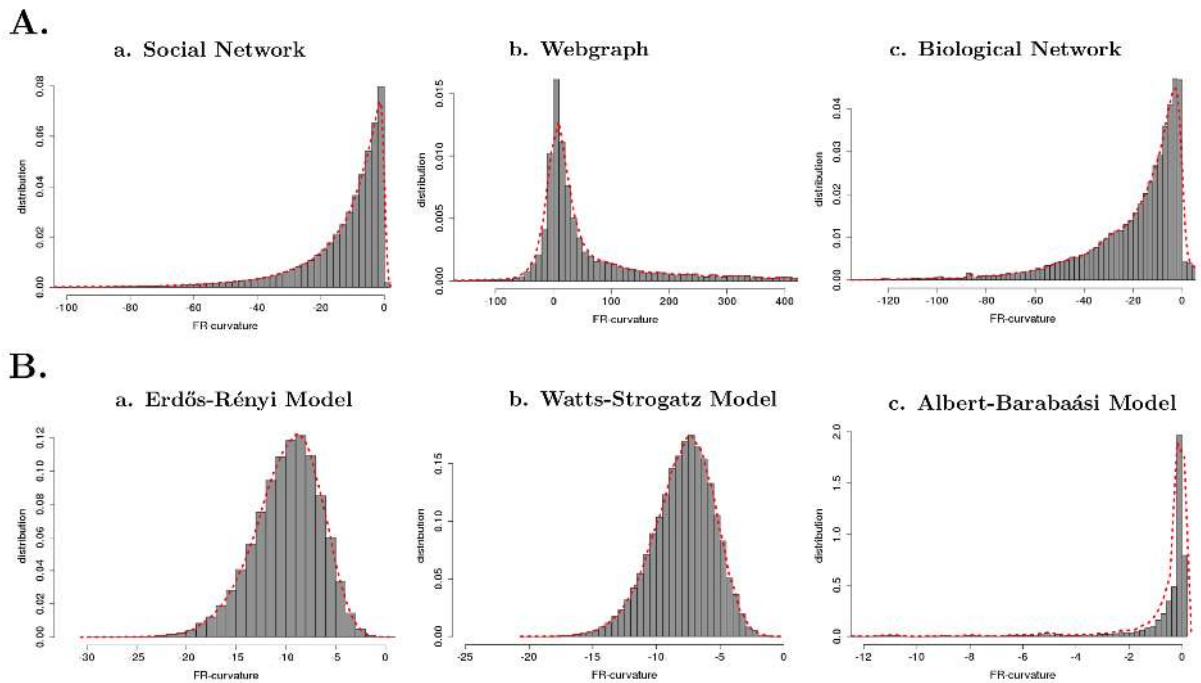

Figure 3: Results for Forman-Ricci curvature: Distributions and density curves. The three real-world examples show a close resemblance with the Albert-Barabási model with the typical power-law distribution. Notably, the width of the distribution is larger than in the case of the AB-model, hinting that real-world-networks are 'mixed types' of model networks, as previously discussed in the literature [Lee et al., 2015].

A comparison of the distributions (Fig.3) indicates strong qualitative similarity between the Albert-Barabási (AB) model and the real-world networks. This hints on a correlation of the curvature distribution and *scale-freeness*, the central property in the AB-model. A more extensive statistical analysis in [Sreejith et al., 2016a, Sreejith et al., 2016b] obtained comparable results, empirically showing a strong correlation between scale-freeness and the distribution of Forman-curvature over a wide range of network examples.

To quantify this observation, we compute the distance between the estimated curvature distributions of our samples and a simulated model network of comparable size. The computation is based on the curvature-based distance introduced in the previous section and utilizes the earth mover's distance determined by the Hungarian algorithm (see *Supplemental Material*). Table 1 summarizes the results. As expected from the qualitative evaluation of the histograms, the

---

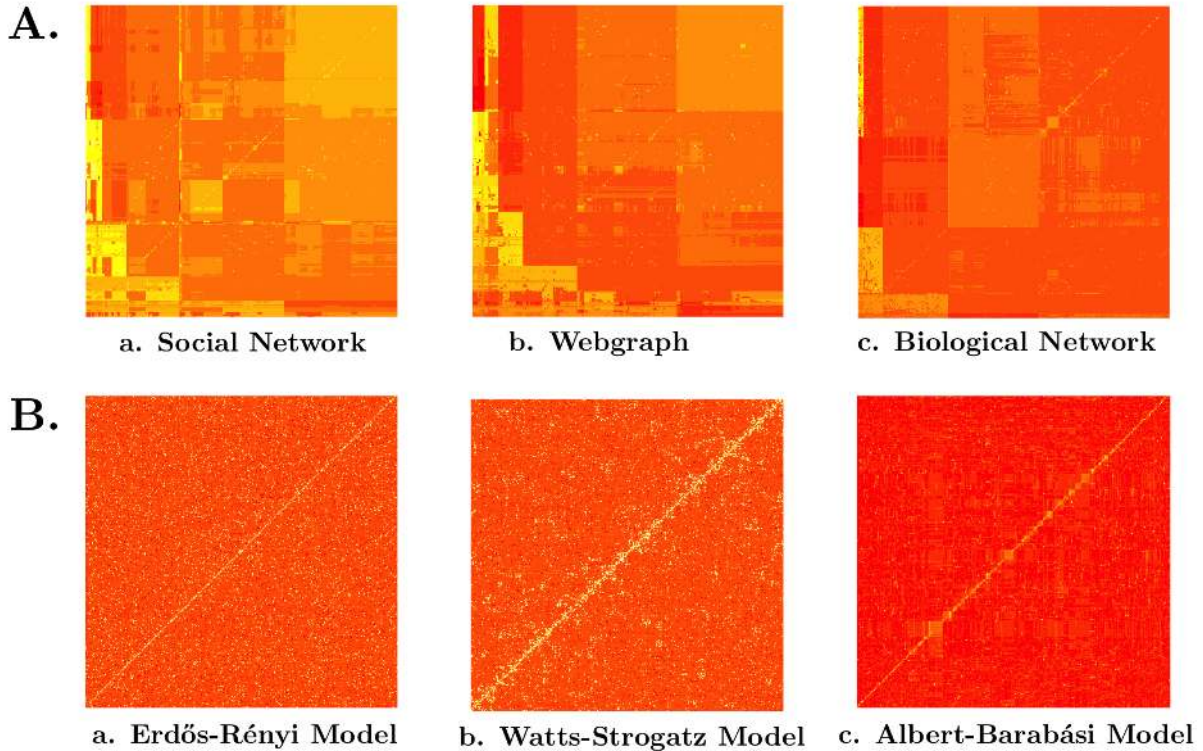[2]see *Supplemental Material* for details on implementation and the publicly available code

Figure 4: Curvature maps for Forman-Ricci curvature. **A:** Curvature maps for subsamples[3] of the three real-world examples with 1,000 nodes. Both the community structure and the directionality of the networks is clearly represented in the maps. **B:** Curvature maps for the three model networks. The Albert-Barabási model (c) shows resemblance with the real-world networks due to its community structure, a result of its intrinsic scale-freeness.

Albert-Barabási model shows by far the most resemblance with the three real-world networks. Surprisingly, our results suggest, that the random graph model (Erdős-Rényi) gives a closer approximation than the Watts-Strogatz model - in contrast to what one would expect from previous studies on other network-characteristics [Newman, 2003]. A closer examination of curvature-distances between a larger number of real-world networks is beyond the scope of this article and remains for future work.

An explanation for the observation of the close resemblance with the Albert-Barabási model follows from the geometric meaning of the curvature: Highly curved edges accumulate in fast evolving network regions that are distinguished by their information content (in the classic Riemannian analogy, large deviations from local flatness of the Euclidean sphere). Previous work in Network Analysis has shown, that major properties of networks are governed by a few densely connected, distinguished nodes (so-called hubs) and the communities of nodes that center around them [Newman, 2006]. This structure is intrinsic to the scale-freeness of the Albert-Barabási-model. Our results suggest, that these hubs and densely connected communities surrounding them, are characterized by high curvature - offering an explanation for the high correlation of curvature distribution and scale-freeness.

Additional insight into the community structure of the networks is gained from evaluating the curvature maps (Fig.4A). The curvature map representation highlights the similiarity of curvature in a specific network region. The rich structure visible in the maps suggests curvature-based clustering as a possible application of the Forman curvature (and the curvature map

13

Network	Curvature-based distance
Facebook (social)	$d_{AB} = 0.0495$
	$d_{WS} = 0.3315$
	$d_{ER} = 0.2706$
Google (web)	$d_{AB} = 0.0546$
	$d_{WS} = 0.3581$
	$d_{ER} = 0.2910$
BioGrid (biological)	$d_{AB} = 0.0604$
	$d_{WS} = 0.2238$
	$d_{ER} = 0.1688$
Distances between	$d(F, G) = 0.0565$
real-world networks	$d(F, B) = 0.0086$
	$d(G, B) = 0.1131$

Table 1: Curvature-based distances between analyzed data sets. The results show, in accordance with our qualitative observations, a close resemblance between the real-world networks and the Albert-Barabási model. The distances among the real-world networks are approximately of the same order.

representation), as we will discuss later in the article.

Curvature maps and Directionality

Furthermore, the curvature maps offer insights into the *directionality* of networks: Undirected networks have symmetric curvature maps; whereas directed ones (as the examples in Fig.4A) are asymmetric. Directionality is an intrinsically edge-based network property that cannot be captured with the standard characteristics. Looking at different classes of real-world networks, including the exemplary ones studied in this article, the great importance of the directionality becomes clear:

Social interactions as well as information flow are rarely symmetric - people in leading positions tend to receive far more emails and status updates from their group members than they send themselves. Hyperlinks between web pages are highly asymmetric as, for instance encyclopedias like Wikipedia link a lot of pages through citations and suggestions for further reading - usually without being linked back by the respective page. Even if links in both directions exist, they need not be used with the same frequency, possibly resulting in different weights. Another example for which directionality is especially well studied, is that of neuronal networks. In characterizing the behavior of neurons as excitatory or inhibitory, opposite signs are assigned to the edge weights - introducing directionality to the network. Furthermore, it is well known that the information flow between different brain regions is highly asymmetric, mostly occurring in only one direction.

Providing a tool to capture and study this intrinsic property of real-world networks is one of the major innovations of the Forman-Ricci curvature. The additional spatial dimension of the curvature maps allows for an elegant representation of directionality and its analysis in terms of community structures.
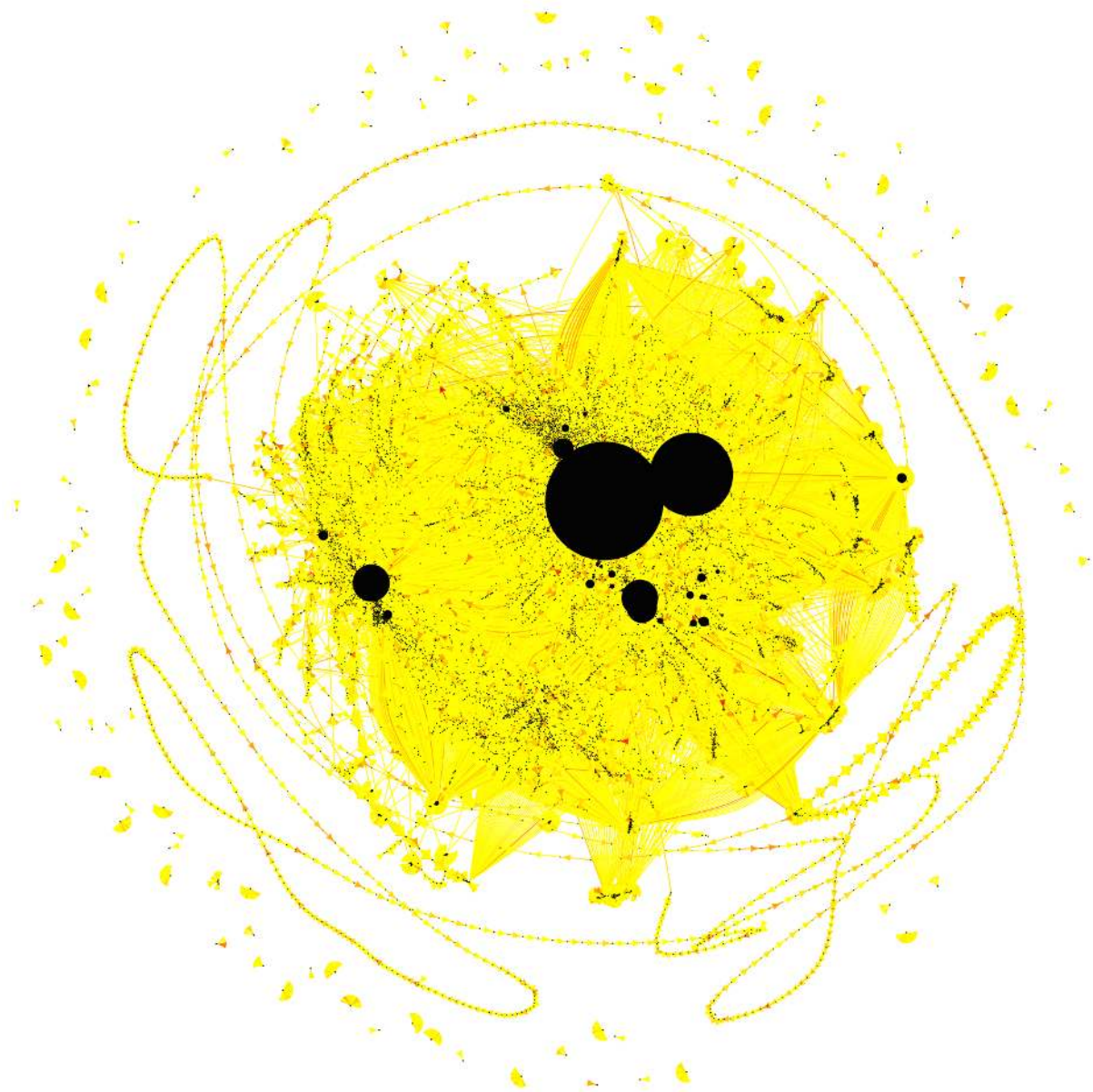
Figure 5: Curvature-colored network plot of a Google webgraph [Kunegis, 2013][Palla et al., 2007].

4 Ricci Flow on networks

The Forman-curvature resides at the base of the very definition of the Forman-Ricci flow and is furthermore closely related to the Laplacian flow. Both flows can be utilized to characterize the dynamics in evolving networks, as we shall see in this section. In this setting, network regions (or communities) with high curvature (in Fig.4: red) are fast evolving, with information flow *towards* (growing with fast accumulation of nodes, positive curvature) or *away from* (shrinking or fast expansion, negative curvature) them. On the contrary, in regions with low curvature (in Fig.4: yellow) the flow is overall low leaving the region static or only slowly evolving.

4.1 Forman-Ricci flow

Pioneered by Hamilton [Hamilton, 1988], and fully developed by Perelman [Perelman, 2002, Perelman, 2003], the Ricci flow has become by now an established and active subject of study

in Differential Geometry – see e.g. [Chow and Knopf, 2004, Topping, 2006] and the references therein.

In the special case of surfaces, the Ricci flow has a very simple and intuitive form, due to an essential identity relating Ricci curvature and the classical Gaussian curvature K, namely:

$$\frac{\partial g_{ij}}{\partial t} = -K(g_{ij}) \cdot g_{ij}; \tag{35}$$

This form of the flow was adapted by Chow and Luo [Chow and Luo, 2003] in their work on the combinatorial Ricci flow on PL surfaces. In turn, it is this equation given in term of the lengths of the edges (1-skeleton) of the given surface that inspired our own definition for dynamically evolving weighted networks in [Weber et al., 2016]:

$$\tilde{\gamma}(e) - \gamma(e) = -\mathrm{Ric}_F(\gamma(e)) \cdot \gamma(e); \tag{36}$$

where $\tilde{\gamma}(e)$ denotes the new (updated) value of $\gamma(e)$ after one time step. Note that in our discrete setting, lengths are replaced by the (positive) edge weights. Time is assumed to evolve in discrete steps and each "clock" has a length of 1.

In contrast, the Forman-Ricci flow based on a discretization of the "proper" 3- (and higher) dimensional flow, i.e.

$$\frac{\partial g_{ij}}{\partial t} = -\mathrm{Ric}(g_{ij}); \tag{37}$$

would give us the following alternative for (36):

$$\tilde{\gamma}(e) - \gamma(e) = -\mathrm{Ric}_F(\gamma(e)). \tag{38}$$

Remark (*Choice of the form of the Ricci flow*). As discussed in [Weber et al., 2016], we consider the Ricci flow in the specific form (36) the Ricci flow has in dimension 2. However, our choice is, by no means, unique. Besides easy computability, a main reason for choosing Eq. 36 is the fact that the most successfull discrete Ricci flow, namely that of Chow and Luo [Chow and Luo, 2003], is of this type.

While defined for triangulated surfaces (i.e. of images), it effectively resides solely on the 1-skeleton, thus providing a formalism that can be easily mapped to the network graphs we are concerned with in the present article. Moreover, this approach is also adopted in defining the only other established Ricci-type flow for networks, namely the *Ollivier-Ricci flow*. It is therefore a natural choice to define a Forman-Ricci flow in a 2-dimensional form, allowing for consistency between and comparison of the two flows. However, note that considering the curvature at the nodes, the Ollivier-Ricci flow represents a *scalar* flow, rather than a Ricci flow [Sandhu et al., 2015a]. In contrast, our proposed form for the Forman-Ricci flow represents a true Ricci flow, since it describes an evolution prescribed by the Ricci curvature of the edges. Thus, it is in concordance with the classical (smooth) Ricci flow.

Another, more theoretical reason for our choice resides in the fact that graphs (and hence networks), while formally 1-dimensional objects, are "almost 2-dimensional". In a sense, they encode in many important cases some essential properties of surfaces [Hua et al., 2015] and, as such, hold in common with 2-dimensional structures many important features. In fact, the

classic 1-dimensional graphs can be extended to higher dimensional structures intuitively, as we will discuss in a follow-up article.

However, beyond this theoretical motivation, practical reason also implies a preference for the form (36): As experiments with images show [Sonn et al., 2014], (38) it is in computational analysis more unstable and tends to produce certain singularities. Given the more discrete nature of networks compared to images, we must expect the flow to be even more prone to such a lack of stability. Therefore, to avoid sharp changes in curvature and weights, it is useful to benefit from the smoothing effect of the edge weight factor in the right side of (36).
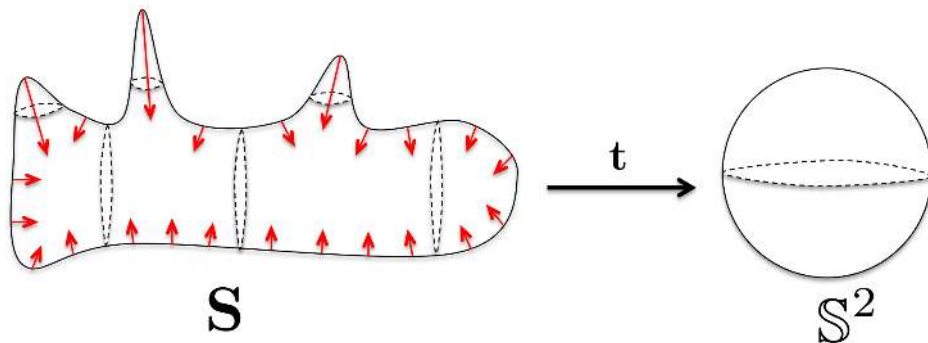

Figure 6: The surface Ricci flow evolves the surface proportionally to the Ricci curvature, towards a gauge surface of constant Gaussian curvature. The spherical form evolves by "pushing" the points of high curvature faster then those of low curvature, such that regions of positive curvature (tend to) shrink, while those of negative curvature (tend to) expand.

The classical Ricci flow for surfaces gives an intuition on the expected properties of the Ricci flow for graphs. More specifically, we expect the surface to evolve through the Ricci flow proportionally to the Ricci curvature towards a model (or "gauge") surface of constant curvature. This intuition is based on the classical case for 3-manifolds, where the Gaussian curvature is in the limit equal to the mean Gaussian curvature of a given surface, i.e. a surface of constant curvature having the same *Euler characteristic* as the original one. This has two aspects:

1. The *short term flow* tends to smoothen the surface by "pushing" the points of high curvature faster then those of low curvature. This suggests some immediate applications of this flow, namely denoising (or – for surfaces – smoothing). Note that Eq. (36) is, in fact an ODE and therefore reversible. The resulting *reverse flow*

$$\frac{\partial \gamma(e)}{\partial t} = +\text{Ric}_F\left(\gamma(e)\right) \cdot \gamma(e) \; ; \tag{39}$$

   can also be exploited for the very opposite goals, e.g. adding of noise (or, in the case of images, sharpening). Such goals are attainable without further theoretical work.

2. One would also like to study the *long term flow*. The motivation for this resides in the hope, that in concordance with the classical Ricci flow for surfaces and with its discrete counterpart introduced by Chow and Luo, the flow will evolve a given network to a *gauge* (or *model*) *network* of a defined topological type (see [Hamilton, 1988], [Chow and Luo, 2003], respectively). However, to avoid the possibility of the network "collapsing" under the flow, one should consider not the standard flow, but rather its *normalized* version. For a surface

this has the following form:

$$\frac{\partial g_{ij}}{\partial t} = - \left(K(g_{ij}) - \overline{K}(g_{ij}) \right) \cdot g_{ij} \, ; \tag{40}$$

where $\overline{K}$ denotes the mean Gaussian curvature of the given surface S^2, namely

$$\overline{K} = \frac{\int_{S^2} K dA}{\int_{S^2} dA} \, ;$$

(dA denoting the area element of S^2).

By analogy with (40) we can define the following *Normalized Forman-Ricci flow* as

$$\frac{\partial \gamma(e)}{\partial t} = \left(\mathrm{Ric}_{\mathrm{F}} \left(\gamma(\mathrm{e}) \right) - \overline{\mathrm{Ric}}_{\mathrm{F}} \right) \cdot \gamma(e) \, . \tag{41}$$

Such a *"gauge" theory* would be extremely important for the study of the evolution of networks and moreover their prediction. Here, we restrict ourselves to empirical tools and thus only perform relevant experiments for the short term flow. In a follow-up article we will attempt to study such *gauge networks* with theoretical tools for higher order network structures. For some additional remarks, see the discussion section of the present paper.

Remark (Metric structure). We note that, while in its present form formally correct and applicable to the cases considered here, an extension to the long term flow is a relevant open point to address in future work. An essential aspect in this context is the introduction of a metric structure: For more rigorously founded geometrical conclusions, such as the evolution of the network under the long term flow, one needs to ensure that the edge weights endow the network with a metric structure. Indeed, without further assumptions, the given weights represent a distance function only on the *star* of a node, i.e. on the edges adjacent to it (and their end nodes). One approach for remediating this issue is the consideration of the *path metric* induced by the given weights.

4.2 Laplacian Flow

Through the *Bochner-Weitzenböck formula*, Forman's Ricci flow is closely related to the *Laplace-Beltrami* (or short *Laplacian*) *flow*. In this section, we want to give a network-theoretic formulation of the Laplacian flow and its relation to the Forman-Ricci flow.

We start with the general notion for Riemannian manifolds and develop a formulation for graphs through an analogy for grids and manifolds that has been successfully applied in Imaging (see, e.g., [Xu, 2004, Kaczynski et al., 2004]).

When considering more general types of surfaces, the general Laplace-Beltrami operator on a Riemannian manifold (M^n, g) is given by ([Berger, 2012]):

$$\triangle_g = \frac{1}{\sqrt{\det(g_{ij})}} \sum_{i,j=1}^{n} \frac{\partial}{\partial x^k} \left(\sqrt{\det(g_{ij})} g^{i,j} \frac{\partial I}{\partial x^l} \right) \, , \tag{42}$$

where $g = (g_{ij})$ and $g^{ij} = g(dx^i, dx^j)$.

Remark. Note, that in contrast to the prevalent convention in Riemannian Geometry, but according to the intuition (and common practice in the Applied Sciences), we have opted for the sign "+" in the definition of the Laplacian, as well as in that of the Ricci flow.

In analogy to a manifold [Xu, 2004, Kaczynski et al., 2004], we consider an image I, viewed as a real, positive function defined on a rectangle (the image base). Then the Laplace-Beltrami flow is defined by

$$\frac{\partial I}{\partial t} = \triangle_g I \, . \tag{43}$$

where $\triangle_g I$ is the standard Laplacian of the metric g of I. The metric g itself is determined by the 1-skeleton of the image, i.e. by the edges between the I-images of adjacent pixels. (For more details see, for instance, [Appleboim et al., 2012] and the references therein.)

Since the edge grid of an image is nothing but a very simple, regular graph, except at the boundary, it is quite natural to extend this type of flow to weighted graphs and networks. We substitute $\triangle_g$ with the Bochner Laplacian obtaining a simplified version of the Laplacian flow for graphs:

$$\frac{\partial G}{\partial t} = \Delta_F^1 G \, . \tag{44}$$

From (44) and from the Forman version of the Bochner-Weitzenböck formula (5), we easily obtain a fitting version for the Laplacian flow on networks:

$$\frac{\partial G}{\partial t} = \Delta_F^1 G = (\square_1 - \mathbf{F})G \, . \tag{45}$$

For the notation in the defining expression (44), we follow the classic convention in Imaging (43). However, note that in practice the flow "resides" on the edges of G, and the evolution of the edge weights therefore intrinsically determines the eventual evolution of the nodes. Note that in both cases the absolute value of the edge weights γ generalize the lengths of the edges (and the metric (g_{ij})). Given (10) and the Bochner Laplacian

$$\square_1(e) = \sum_{e \sim v} \frac{\omega(v)}{\gamma(e)} \, ; \tag{46}$$

from (12), we can calculate the Laplacian flow, according to (45).

4.3 Characterizing dynamic effects in networks

Detection of changes and "interesting" regions with Forman-Ricci flow

In [Weber et al., 2016], we introduced a formalism for characterizing dynamics in complex networks. We will review the mathematical details here and then perform a more sophisticated dynamic analysis of the Gnutella network [Leskovec and Krevl, 2014], [Leskovec et al., 2007], [Ripeanu et al., 2002], going well beyond the investigations in [Weber et al., 2016].

The Ricci flow based on Forman curvature provides a tool for studying dynamic effects, resulting from information flow, in complex networks. For this, we consider a set of 'snapshots' that specify the network's structure (connections between nodes and their strength) at given (discrete) time points $\{t_i\}$ represented as weighted graphs $(G_i)_{i \in I}$. By analyzing the flow of the curvature between the time points, we gain insights into structural changes that can be utilized

in a number of applications, as discussed below.

For computing the flow, we consider the following formalism: Let t_i and t_{i+1} be adjacent time points with corresponding graphs G_i and G_{i+1}. The Forman-curvature characterizes the geometric structure of G_i and G_{i+1} based on the weighting schemes

$$\omega^0_{n,n+1} : V(G) \mapsto [0,1] \,, \tag{47}$$

and edges

$$\gamma^0_{n,n+1} : E(G) \mapsto [0,1] \,, \tag{48}$$

at times t_i and t_{i+1}. From this, we compute the Ricci flow Eq. (36) at $\Delta t = t_{i+1} - t_i$ by iterating $k = 1, ..., K$ times:

$$\gamma^{k+1}_{i,i+1}(e) = \gamma^k_{i,i+1}(e) - \Delta t \cdot \mathrm{Ric}_F(\gamma^k_{i,i+1}(e)) \cdot \gamma^k_{i,i+1}(e) \,. \tag{49}$$

resulting in updated weighting schemes γ^K_i and γ^K_{i+1}. The correlation between the updated weights is a measure of the flow Eq. (49), identifying network regions that have undergone significant structural changes at Δt by evaluating the corresponding (thresholded) correlation matrix. Alternatively, one can align the edges of G_i and G_{i+1} beforehand and compare the distance between the edge weights (using the L^1-norm). We will use the later one here, for the correlation-approach see [Weber et al., 2016].

For computing[4] the Ricci flow, we use the following work flow:

1. Calculate the Forman-Ricci curvature for the network's states at times t and $t + \Delta t$ (e.g. version of a data base, downloaded at t_i and its preceeding version from $t_{i+1} = t_i + \Delta t$).

2. Normalize the networks, i.e. the updated weighting schemes γ^k_i and γ^k_{i+1}.

3. Calculate the discrete Ricci flow for each network through iteration over

$$\gamma^{k+1}_{ij} = \gamma^k_{ij} - \Delta t \cdot Ric(\gamma^k_{ij}) \,.$$

Fig. 7 shows the detection of fast evolving edges and, more broadly, the identification of "interesting" dynamically changing regions. The capability of the Ricci flow to detect such regions relates to our observations on the Forman-Ricci curvature in static networks in the previous section: Hubs in dense network regions (communities) govern the global properties of the network through strong connections with their neighbors. Those strong connections are characterized by high (absolute) Forman curvature, which is by its very definition, related to network growth. Regions of high curvature are therefore fast evolving, the respective changes in edge weights – characterized by the Ricci flow – describe the growth or shrinkage behavior.

Denoising with Laplacian flow

Networks built from empirical data, such as the ones considered in the previous section, are greatly affected by noise in the underlying data. Especially sensitive are the edge weights

---

[4]see *Supplemental Material* for details on implementation and the publicly available code

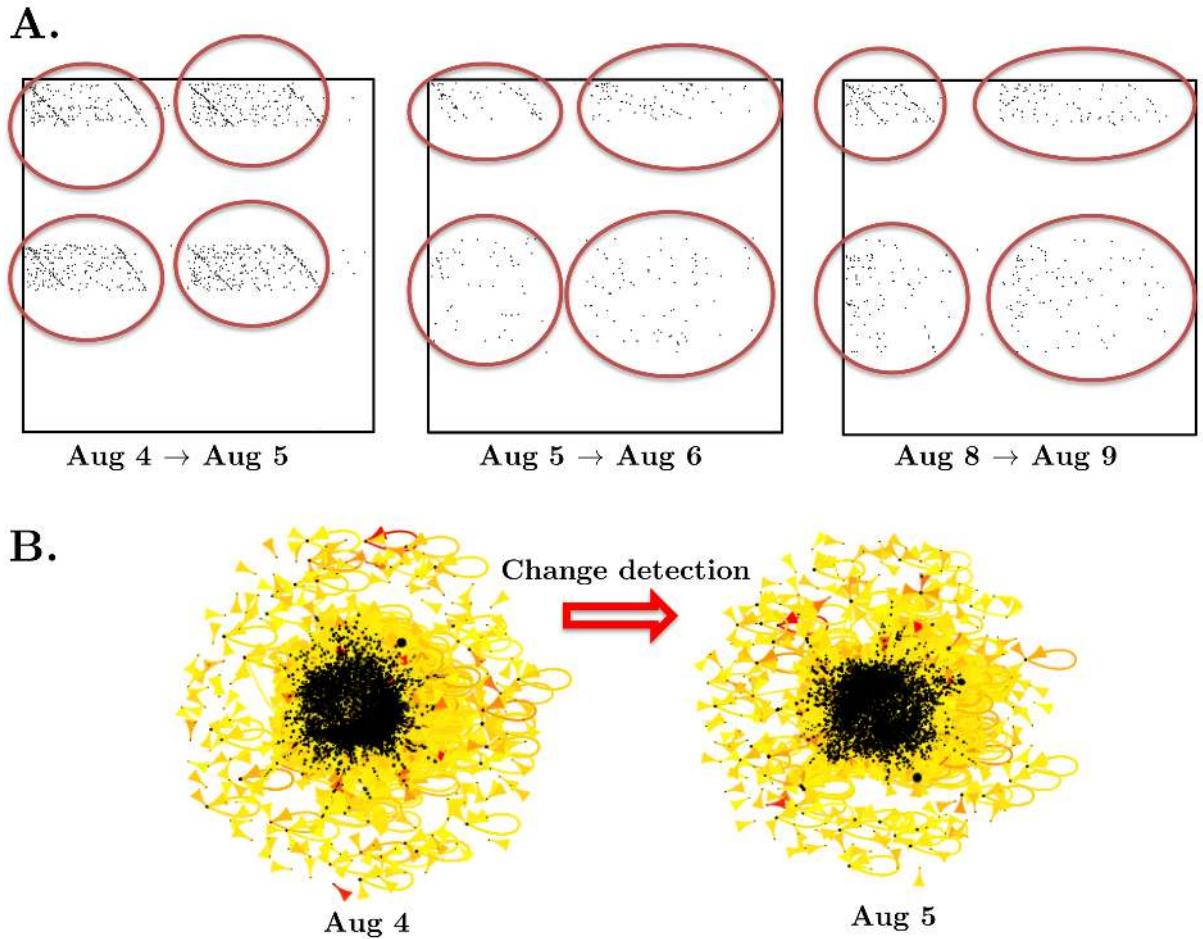Figure 7: Characterization of information exchange in Gnutella. **A:** Change detection with Forman-Ricci flow and L^1-distance (K=10, threshold=0.1). **B:** Graph plot of Gnutella information (August 4 and August 5 2012). Edges are colored according to their Forman-Ricci curvature.

that describe the strength of the inferred associations. Utilizing the *averaging effect* of the Laplacian flow, we propose a method for correction of arbitrary small fluctuations as a first step towards denoising networks. When inferring a network from given data, and assuming, that small fluctuations mainly affect the strength of the edges and not their existence itself, one gets

$$\tilde{G} = \{V, E, \omega, \tilde{\gamma}\} \, , \tag{50}$$

Under this assumption, we can limit our analysis to the denoising of the edge weights, i.e. construct γ from $\tilde{\gamma}$:

$$\tilde{\gamma} = \gamma + dt \cdot dW \, . \tag{51}$$

We assume arbitrary small fluctuations of the form of *Gaussian white noise dW* and attempt to smooth the resulting noise effects with the Laplacian flow:

$$\gamma \approx \tilde{\gamma} - dt \cdot \Delta_F^1(G) \, . \tag{52}$$

This formalism is restricted to cases where the correction term is small with respect to the edge

weights. Additionally, we only consider the short term flow, assuming that the fluctuations are mainly a result of spontaneous irregularities that occur over a short term.

With the corrected weights γ, we can reconstruct the denoised graph as

$$G = \{V, E, \omega, \gamma\} . \tag{53}$$

Fig.8 shows the correction of fluctuations in the edge weights with the Laplacian flow for a small use case. The intuitive scheme of the method can be easily extrapolated to large networks. The distance between the original and the corrected weights (i.e. the *denoising level*) can be calculated using the L^1-norm, since the edges are aligned. First (preliminary) computational tests on a selected set of real-world networks showed promising results.
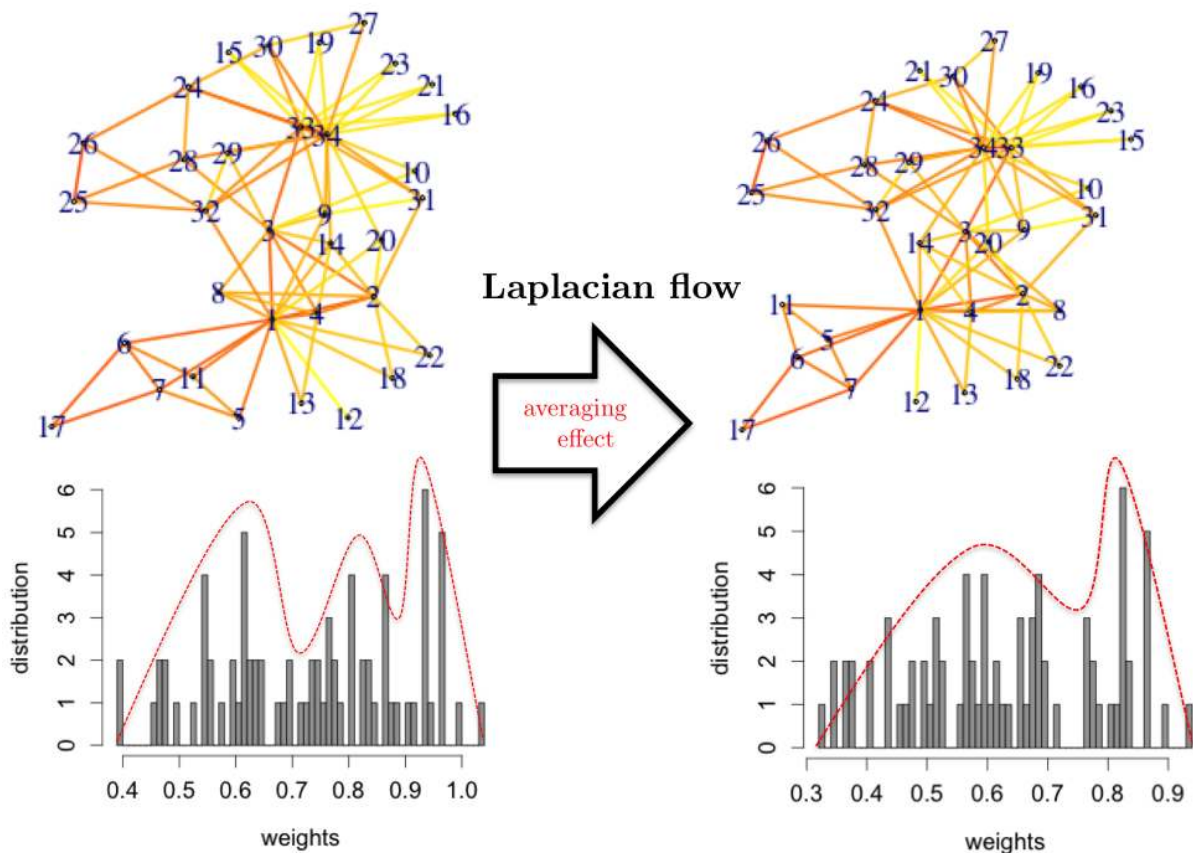

Figure 8: Denoising with Laplacian flow. The *averaging effect* of the Laplacian flow smoothes the distribution of edge weights and corrects for small fluctuation and random noise in the underlying data (here: Zachary's karate club [Zachary, 1977]). For illustration, we highlight the averaging effect schematically.

4.4 Duality of Ricci curvature and the Laplacian

The derivation of the definition of the Forman-Ricci curvature (9) from the Bochner-Weitzenböck formula (5) introduces a deep theoretical insight: It connects the curvature of the manifold to the Riemann-Laplace operator, hence to the heat diffusion. Loosely formulated, the Laplacian flow incorporates both an "approximate", or rough Laplacian, as well as a correcting geometric component, namely the curvature term. In consequence, the Laplacian flow captures the behavior of both the Laplacian on and the curvature of the underlying manifold. Note that only for

the case $p = 1$, i.e. for the Ricci curvature, the curvature term has a clear and specific geometric content.

Moreover, the importance of the observation above is not restricted to the theoretical realm, but has concrete and meaningful practical consequences. Indeed, the fact that one can obtain, through Forman's method [Forman, 2003], both a Ricci curvature and a Laplacian, endows us with the discretization of two powerful geometric, respective analytic, tools, that have found a wide range of applications in various fields of Computer Science. In particular, one can consider not just the Forman-Ricci flow introduced above, but also a fitting discretization of the Laplacian flow, which we discuss in more detail below.

However, let us first emphasize the main significance of this *duality* between curvature and Laplacian. Clearly, it allows us to define discrete, network-theoretic versions of both the Ricci and the Laplacian flow. This, in turn, allows for capturing a number of network properties through the specific characteristics of the two flows.

Curvature and, in particular, Ricci curvature, is an edge-based network characteristic and therefore naturally associated with the edge structure and contours of the system characterized by sharp changes in curvature. The corresponding Forman-Ricci flow is expected to identify the equivalent of such features, i.e. regions where curvature changes abruptly over a short time. Those defining features act as the "backbone" of the network, providing a dense synopsis of its topology and structural information. We refer to this intrinsic property of the Forman-Ricci flow as *backbone effect*. It was this very behavior of the short term Ricci flow that we exploited in [Weber et al., 2016] when first introducing the change detection method.

On the other hand, the Laplacian flow has a strong *averaging* or *smoothing effect* that is intuitively implied by its origins in the heat equation. It has been successfully applied for smoothing and filtering of noise in Imaging (see e.g. [Appleboim et al., 2012], [Sonn et al., 2014]). In an attempt to correct for small fluctuations in networks built from noise-effected empirical data, we transferred this property to networks, with the same noise-reducing effect.

Computational experiments using the respective other flow yielded less promising results. Especially the Laplacian flow seems, due to its strong smoothing effect, ill-suited for the detection of sharp increases in curvature as utilized in the change detection method. Furthermore, we note that in their discrete versions, the defining equations of both the Ricci and the Laplacian flows are reversible. This is of practical importance for the first introduced method of change detection, considering that a specific reverse flow (i.e. endowed with "-" sign) provides a tool for different applications than the original one (with the "+" sign). In particular, the reverse $\square_1$ flow functions as sharpening operator, whereas the direct flow $\square_1$ provides an efficient anomaly detection tool.

5   Discussion

In this article, we applied Forman's Ricci curvature and Bochner Laplacian [Forman, 2003] to networks and examined their capabilities as network characteristics. We found, that additional structural information is encoded in the edge weights, which is difficult to evaluate using the established node-based characteristics. This shortcoming affects especially the directionality of edges that is of high importance in the analysis of many real-world networks. The curvature

maps introduced in this paper allow for representation of directionality, possibly providing insights into the information flow and evolutionary behavior of densely interconnected subgraphs (communities).

A comparison of our results for three real-world networks with established model networks confirmed the observation in earlier work [Sreejith et al., 2016a, Sreejith et al., 2016b] of a close resemblance in the curvature distribution of real-world networks and the Albert-Barabási-model. We extended the statistical approach therein by introducing a curvature-based distance measure between graphs utilizing the earth mover's distance between the respective curvature density estimates. This formalism gives rise to a classification scheme for networks based on Forman-Ricci curvature as we demonstrated for a small set of samples.

One could argue that there are other approaches to define a curvature on networks than Forman's that have been studied more intensely, including Ollivier's [Li et al., 2014, Ni et al., 2015, Sandhu et al., 2015b]. One caveat of Forman's curvature in relation to Ollivier's resides in its intrinsic local definition being defined only for edges, i.e. adjacent pairs of nodes. However, one can construct order-2, -3, etc. *neighbourhood graphs* by connecting all nodes that are at combinatorial distance 2 from the given node. The weight associated to this "order 2" edge would be the sum of the weights of the composing (original) edges (for the combinatorial distance this would equal 2). Now one can compute the Forman curvature of the resulting weighted graph. In addition, there are strong indications that Forman's and Ollivier's curvature are closely interrelated (as we shall shortly show in a forthcoming study). While measuring similar aspects of network topology, Forman's is, however, much easier and efficient to compute. This is especially important for the typically large networks relevant for applications to real-world complex systems.

In the second part of the article, we extended our approach to dynamic networks by applying the Forman-Ricci flow - based on Forman's Ricci curvature - to networks. We introduced a method to detect changes in an evolving network. Furthermore, we suggested the Laplacian flow as a tool for denoising networks built from empirical data.

While only theoretically proposed and illustrated solely on a small example in this work, a number of practical applications follow immediately from the theoretical results:

1. **Classification**

   In the second section we introduced a curvature-based distance measure that quantifies the dissimilarity between a pair of graphs. Naturally, this distance gives rise to a classification scheme. We were able to reproduce and quantify previous statistical results in [Sreejith et al., 2016a, Sreejith et al., 2016b, Weber et al., 2016], that demonstrated a strong similarity between different classes of real-world networks and the Albert-Barabási model network. A more extensive study of a larger number of data sets and comparison with various model networks remains subject to future work.

2. **Detection of "interesting" regions**

   The Ricci flow characterizes regions of significant dynamic changes in the curvature, hinting on structural changes in the underlying system. Looking at the flow over the course of time, regions of ongoing changes are likely to contain significant information about the

system and its dynamics. Therefore, the flow provides a tool for identifying "interesting" regions that are worth a closer analysis. We outlined the respective computational tools and demonstrated their abilities on a use case. Further study and a statistical analysis of a larger set of test samples is left for future work.

3. **Network extrapolation**

   From knowledge of the flow over a given time range, one could extrapolate the dynamics of past and future time points. In analogy to the flow in the physical sense, one could model the flow with common equations of motion, yielding approximations of the long-term development of the network and prediction of future network states. For this, one would need to extend the assumption of short-term flows, used in the present article for the sake of simplicity, to the long term case. We only aimed to lay a theoretical fundament for curvature-based network extrapolation leaving extended studies for future work. To utilize the full potential of such a long-term flow, one needs to consistently define the "gauge" networks mentioned when discussing the normalized flow. One serious impediment to this endeavor resides in the fact that the Forman-Ricci curvature does not satisfy a Gauß-Bonnet type theorem, thus – in contrast with the surface case – no clear topological class can be assigned to a gauge network. In a forthcoming article by the authors we will show how one can remedy this drawback and indeed define a long time Forman-Ricci flow.

4. **Clustering**

   The curvature maps introduced in section two strongly suggested a relation between community structure and curvature clusters. This is an argument for the application of community detection algorithms to the curvature distribution across the network in an attempt to improve existing clustering tools. A future computational method using this approach could build on earlier, related work for genetic networks [Saucan and Appleboim, 2005]. For now, it remains a subject for future work.

5. **Denoising**

   A natural application of the geometric flows associated with Forman-Ricci curvature is denoising. Empirical results in related fields, particularly Graphics and Imaging, suggest that the Laplacian flow gives good results for denoising. We transfer this idea to the network-theoretic Laplacian flow introduced in the present paper and perform a similar analysis for denoising of networks built from (noise-affected) empirical data. The promising results obtained for test cases motivate the further exploration of this idea in the future.

We showed, that Forman's theoretical work [Forman, 2003] allows for defining both the Ricci and the Laplacian flow for network in an intuitive and efficiently computable way. The applications proposed above utilize the intrinsic strengths of both flows: The *backbone effect* of the Ricci flow allowing for identification of defining properties and dynamics, and the *averaging effect* of the Laplacian flow capable of smoothing and correcting small irregularities in the underlying empirical data. The existence of these two complementary characteristics and their strong relation through the *Bochner-Weitzenböck-formula* offers a rich basis for dynamic network analysis.

This article presents a curvature-based approach to characterize networks adding an edge-based

characteristic to the established network-analytic "toolbox". Building on and extending previous work of the author and the group, we presented the mathematical motivation of the curvature-based approach and provided examples for different types of real-world complex networks. Furthermore, we propose a number of practical applications, specifically utilizing Forman's Ricci flow that will be extended in future work.

With our work we hope to add to the common effort of developing new network-analytic tools for handling the challenges in data science come with the increasing amount of available data and the recent rapid development of the field.

6   Acknowledgements

Supplemental Material

Supplement 1: Sampling of large networks.
Supplement 2: Approximation of EMD with total variation.
Supplement 3: Implementation of curvature and Laplacian analysis.
Supplement 4: Data sets.

References

[Amaral et al., 2000] Amaral, L. A. N. et al. (2000). Modes of interaction between individuals dominate the topologies of real world networks. *PNAS*, 97(21):11149–11152.

[Appleboim et al., 2012] Appleboim, E., Saucan, E., and Zeevi, Y. Y. (2012). Ricci Curvature and Flow for Image Denoising and Superesolution. *Proceedings of EUSIPCO*, pages 2743–2747.

[Arita, 2004] Arita, M. (2004). The metabolic world of Escherichia coli is not small. *PNAS*, 101(6):1543–1547.

[Ballouz et al., 2016] Ballouz, S., Weber, M., Pavlidis, P., and Gillis, J. (2016). Egad: Ultra-fast functional analysis of gene networks. *bioRxiv:053868*.

[Banerjee and Jost, 2008] Banerjee, A. and Jost, J. (2008). Spectral plot properties: Towards a qualitative classification of networks. *Networks and heterogeneous media*, 3(2):395–411.

[Barabási and Albert, 1999] Barabási, A. L. and Albert, R. (1999). Emergence of scaling in random networks. *Science*, 286(5439):509–512.

[Bauer et al., 2012] Bauer, F., Jost, J., and Liu, S. (2012). Ollivier-Ricci curvature and the spectrum of the normalized graph laplace operator. *Mathematical research letters*, 16:1185–1205.

[Berger, 2012] Berger, M. (2012). *A Panoramic View of Riemannian Geometry*. Springer, Berlin (Germany).

[Chow and Knopf, 2004] Chow, B. and Knopf, D. (2004). The Ricci Flow: An Introduction. *Mathematical Surveys and Monographs*, 110.

[Chow and Luo, 2003] Chow, B. and Luo, F. (2003). Combinatorial Ricci flows on surfaces. *Journal of Differential Geometry*, 63(1):97–129.

[Eckmann, 1944] Eckmann, B. (1944). Harmonische Funktionen und Randwertaufgaben in einem Komplex. *Comment. Math. Helv.*, 17(1):240–255.

[Erdős and Rényi, 1959] Erdős, P. and Rényi, A. (1959). On Random Graphs I. *Publicationes Mathematicae*, 6:290–297.

[Erdős and Rényi, 1960] Erdős, P. and Rényi, A. (1960). On the evolution of random graphs. *Publicationes Mathematicae*, 5:17–61.

[Forman, 2003] Forman, R. (2003). Bochner's Method for Cell Complexes and Combinatorial Ricci Curvature. *Discrete and Computational Geometry*, 29(3):323–374.

[Gibbs and Su, 2002] Gibbs, A. L. and Su, F. E. (2002). On Choosing and Bounding Probability Metrics. *International Statistical Review*, 70(3):419–435.

[Gu et al., 2016] Gu, J. et al. (2016). Spectral classes of regular, random and empirical graphs. *Linear algebra and its applications*, 489:30–49.

[Hamilton, 1988] Hamilton, R. S. (1988). The Ricci flow on surfaces (at Mathematics and general relativity, Santa Cruz CA). *Contemp. Math.*, 71:237–262.

[Horak and Jost, 2013] Horak, D. and Jost, J. (2013). Spectra of combinatorial Laplace operators on simplicial complexes. *Advances in Mathematics*, 244:303–336.

[Hua et al., 2015] Hua, B., Jost, J., and Liu, S. (2015). Geometric analysis aspects of infinite semiplanar graphs with nonnegative curvature. *Journal für die reine und angewandte Mathematik (Crelles Journal)*, 700:1–36.

[Jeong et al., 2000] Jeong, H. et al. (2000). The large-scale organization of metabolic networks. *Nature*, 407:651–654.

[Jost, 2011] Jost, J. (2011). *Riemannian Geometry and Geometric Analysis*. Springer, Berlin (Germany).

[Jost and Liu, 2014] Jost, J. and Liu, S. (2014). Olliviers Ricci curvature, local clustering and curvature-dimension inequalities on graphs. *Discrete and Computational Geometry*, 51(2):300–322.

[Kaczynski et al., 2004] Kaczynski, K., Mischaikow, K., and Mrozek, M. (2004). *Computational homology*. Springer, New York (USA).

[Kunegis, 2013] Kunegis, J. (2013). KONECT - The Koblenz Network Collection. *Proc. Int. Web Observatory Workshop*, pages 1343–1350.

[Lee et al., 2015] Lee, I., Kim, E., and Marcotte, E. M. (2015). Modes of interaction between individuals dominate the topologies of real world networks. *PlosOne*, 10(3).

[Leskovec et al., 2007] Leskovec, J., Kleinberg, J., and Faloutsos, C. (2007). Graph Evolution: Densification and Shrinking Diameters. *ACM Transactions on Knowledge Discovery from Data (ACM TKDD)*, 1(1).

[Leskovec and Krevl, 2014] Leskovec, J. and Krevl, A. (2014). SNAP Datasets: Stanford Large Network Dataset Collection.

[Li et al., 2014] Li, W. et al. (2014). Optimal Transport in Worldwide Metro Networks. *preprint, arXiv:1403.7844*.

[Loisel and Romon, 2014] Loisel, B. and Romon, P. (2014). Ricci curvature on polyhedral surfaces via optimal transportation. *Axioms*, 3:119–139.

[McAuley and Leskovec, 2012] McAuley, J. and Leskovec, J. (2012). Learning to Discover Social Circles in Ego Networks. *NIPS 2012*.

[Newman, 2003] Newman, M. E. J. (2003). The structure and function of complex networks. *SIAM Review*, 45(2):167–256.

[Newman, 2006] Newman, M. E. J. (2006). Modularity and community structure in networks. *PNAS*, 103(23).

[Ni et al., 2015] Ni, C. et al. (2015). Ricci curvature of the internet topology. *IEEE Proceedings of INFOCOM*, pages 2758–2766.

[Ollivier, 2009] Ollivier, Y. (2009). Ricci curvature of Markov chains on metric spaces. *Journal of Functional Analysis*, 256(3):810–864.

[Ollivier, 2010] Ollivier, Y. (2010). A survey of Ricci curvature for metric spaces and Markov chains. *Probabilistic approach to geometry*, 57:343–381.

[Palla et al., 2007] Palla, G. et al. (2007). Directed network modules. *New J. Phys.*, 9(6):186f.

[Perelman, 2002] Perelman, G. (2002). The entropy formula for the Ricci flow and its geometric applications. *preprint, arxiv:math.DG/0211159*.

[Perelman, 2003] Perelman, G. (2003). Ricci flow with surgery on three manifolds. *preprint, arxiv:math.DG/0303109*.

[Ripeanu et al., 2002] Ripeanu, M., Foster, I., and Iamnitchi, A. (2002). Mapping the Gnutella Network: Properties of Large-Scale Peer-to-Peer Systems and Implications for System Design. *IEEE Internet Computing Journal*.

[Rubner et al., 2000] Rubner, Y., Tomasi, C., and Leonidas, J. G. (2000). The earth mover's distance as a metric for image retrieval. *International Journal of Computer Vision*, 40(2):99–121.

[Sandhu et al., 2015a] Sandhu, R. et al. (2015a). Graph curvature for differentiating cancer networks. *Scientific Reports*, 5.

[Sandhu et al., 2015b] Sandhu, R., Georgiou, T., and Tannenbaum, A. (2015b). Market fragility, systemic risk, and Ricci curvature. *preprint, arXiv:1505.05182*.

[Saucan and Appleboim, 2005] Saucan, E. and Appleboim, E. (2005). Curvature based clustering for DNA microarray data analysis. *Lecture Notes in Computer Science (LNCS)*, 3523:405–412.

[Sonn et al., 2014] Sonn, E. et al. (2014). Ricci Flow for Image Processing. *Proceedings of IEEEI 2014*.

[Sreejith et al., 2016a] Sreejith, R. P. et al. (2016a). Forman curvature for complex networks. *Journal of Statistical Mechanics: Theory and Experiment (JSTAT)*.

[Sreejith et al., 2016b] Sreejith, R. P. et al. (2016b). Forman curvature for directed networks. *preprint, arXiv:1603.00386*.

[Stark et al., 2006] Stark, C. et al. (2006). BioGRID: a General Repository for Interaction Datasets. *Nucleic Acids Research*, 34(1):535–539.

[Stone, 1976] Stone, D. A. (1976). A combinatorial analogue of a theorem of Myers. *Illinois Journal of Mathematics*, 20(1):12–21.

[Strogatz, 2006] Strogatz, S. H. (2006). Exploring complex networks. *Nature*, 410:268–276.

[Topping, 2006] Topping, P. M. (2006). Lectures on the Ricci Flow. *London Mathematical Society Lecture Note Series*, 325.

[Watts and Strogatz, 1998] Watts, D. J. and Strogatz, S. H. (1998). Collective dynamics of 'small-world' networks. *Nature*, 393(6684):440–442.

[Weber et al., 2016] Weber, M., Jost, J., and Saucan, E. (2016). Forman-Ricci flow for change detection in large dynamic data sets. *to appear in: Proceedings of ICICS 2016, arXiv:1604.06634*.

[Xu, 2004] Xu, G. (2004). Discrete Laplace-Beltrami operators and their convergence. *Computer Aided Geometric Design*, 21:767–784.

[Yin et al., 2008] Yin, X. et al. (2008). Discrete Curvature Flow for Hyperbolic 3-manifolds. *Emerging Trends in Visual Computing*, 5416:38–74.

[Zachary, 1977] Zachary, W. W. (1977). An information flow model for conflict and fission in small groups. *Journal of Anthropological Research*, 33:452–473.